Journal of the Korean Physical Society, Vol. 40, No. 5, May 2002, pp. 856∼860

Measurement of the Non-Thermal Properties in a Low-Pressure Spraying Plasma

Yong Ho JUNG* and Kyu-Sun CHUNG
Department of Nuclear Engineering, Hanyang University, Seoul 133-791

(Received 4 March 2002)

The non-thermal properties of a low-pressure spraying plasma have been characterized by using optical emission spectroscopy and single probes installed in a fast scanning probe system. A two-temperature model of the electrons is introduced to explain their non-isothermal properties, which are measured using single probes. The excitation temperatures of the atomic and the ionic lines are calculated from measurements of the emission intensities of Ar (I) and Ar (II), and those temperatures can be explained by using a local thermodynamic equilibrium (LTE) or a non-local thermodynamic equilibrium (non-LTE) model. In order to deduce more reasonable values (excitation temperatures), we introduce a multi-thermodynamic equilibrium (MTE) model, which gives different temperatures, depending upon the atomic excitation states.

PACS numbers: 52.70.Ds, 52.75.Hn, 52.70.Kz
Keywords: Spraying plasma, Single probe, Optical emission spectroscopy, Electron temperature, Plasma density, Excitation temperature, Partical local thermodynamic equilibrium, Multi-thermodynamic equilibrium, Two-temperature model

I. INTRODUCTION

Spraying plasmas generated by thermal ionization of plasmas are applied to the following [1–7]: welding, cutting, surface hardening, manufacture of microstructure ceramic powders, iron manufacture, smelting, heating of blast furnaces, superconducting thin films, diamond synthesis, crystal growth, ceramic sintering, gasification of coal by thermal decomposition, decomposition of automobile exhaust fumes, and waste disposal. They are characterized by low electric fields (E), high pressures (P) ($E \leq 10^4$ V/m and $E/P < 3$ V/mPa) [6], and small size (∼1 cm in radial length, 3∼10 cm in axial length). In spite of the small size, the temperature and density variations are very severe, 1,000∼20,000 K and 10^{15}∼10^{16} cm^{-3}. The energy distributions of the particles (electrons, ions, atoms and molecules, *etc.*) are assumed to be Maxwellian, but non-Maxwellian distributions are possible because of the rapid density variation. If the plasma density is over 10^{16} cm^{-3}, the temperatures of electron (T_e) and other particles (T_h) are about the same; namely, all particles are in a state of thermal equilibrium. If plasma density is under 10^{16} cm^{-3}, the electron temperature is higher than those of other particles.

Behavior of a thermal plasma is mainly controlled by the flow velocity, the density, and the temperature of the particles, and these variables affect the characteristics of a plasma-spraying system. Therefore, the speed, the size and the surface temperature distribution of the spraying particles play decisive roles in understanding energy, momentum, and mass transport between plasmas and particles, and these parameters become essential variables necessary to design a plasma-spraying system. Measurements of the plasma density, temperature, and flow velocity can be done by using optical emission spectroscopy, electric probes, and laser interferometers, by which the ion and electron temperatures are deduced under the assumption of local thermodynamic equilibrium (LTE) and an isothermal electron distribution. For the case of an atmospheric spray, the LTE model can be applied to plasmas at the nozzle entrance and to those on the axis of the plasma flame, but it is not easy to justify applying the LTE model to an off-center plasma and to a low-pressure spraying plasma. Wiese *et al.* found non-LTE effects in an atmospheric hydrogen arc and suggested that non-LTE effects may contribute to variations in the atomic transition probability (A_{mn}) for the Ar(II) 480.6 nm line [8,9].

Various diagnostic and analyzing methods can be used to determine if non-LTE properties exist in spraying plasmas. One of them is based on a two-temperature model for the electron temperature and a different gas temperature (T_g) in the spraying plasma while the partial-LTE model assumes that the electron temperature equals upper level excitation temperature (T_{ex}). The partial-LTE model has been shown to contradict itself experimentally when appropriate models are applied [10]. On the other hand, multi-temperature models, which set a dif-

*E-mail: yhjung@ihanyang.ac.kr

ferent temperature to each species, have been treated as a multi-thermodynamic equilibrium (MTE) model [11].

It is the purpose of this work to measure the non-isothermal properties of electrons and to investigate the non-LTE model of the spraying plasma in a low-pressure plasma-spraying system. The non-isothermal properties of the electrons are measured based upon two-temperature model, which is deduced from electron energy distribution function (EEDF) by using a fast scanning probe system (FSPS) with a single probe installed. The non-LTE model will be analyzed by using the excitation temperatures of the ions and the neutral particles, which are deduced from partial-LTE and MTE models through calculations of the intensities of the spectral lines emitted from the plasma detected by using optical emission spectroscopy.

II. THEORITICAL BACKGROUND

1. Single Probe

A single probe can measure the plasma density, temperature, and potential by analyzing the current collected by the probe for a specific applied voltage. The deduction of the plasma parameters strongly depends upon the collisionality of the charged particles [12], *i.e.*, collisionless ($\lambda > (a + \chi_s)$) and collisional ($\lambda < (a + \chi_s)$), where λ is the mean free path of the charged particles, a is the probe radius, and χ_s is the sheath thickness. For the case of a collisionless plasma, if $\chi_s < a$, the probe data are generally to be interpreted by using a Child-Langmuir law [12] while the orbital motions of the ions must be considered if $\chi_s > a$. Even for the collisional plasma, if $\chi_s < a$, the current density collected by the probe, according to the research results of Chen [12] and Hutchinson [13], is reduced as follows:

$$\Gamma = \frac{1}{4} n_\infty \bar{v} \frac{1}{1 + 3a/4\lambda} \approx \frac{1}{4} n_\infty \bar{v} \frac{4\lambda}{3a} \quad for\ a/\lambda \gg 1, \tag{1}$$

where Γ is the flux density, n_∞ is the unperturbed density, and $\bar{v}$ is the mean speed. If $\chi_s > a$, sheath expansion is accompanied by an increased ion saturation current to the probe [14]. Because the working pressure of gas generally affects λ, the plasma density must be changed in consideration of the collisionality of the plasma when the working pressure is high. We can classify plasmas in six types [14,15] according to a and λ as follows:

Case I. $a/\lambda < 1$: Conventional Langmuir Probe,
(a) $4\lambda_D < a < \lambda$ (collisionless thin sheath),
(b) $a < 4\lambda_D < \lambda$ (collisionless thick sheath),
(c) $a < \lambda < 4\lambda_D$ (collisional thick sheath: hybrid case),
Case II. $a/\lambda > 1$: Continuum Electrostatic Probe,
(a) $\lambda < 4\lambda_D < a$ (collisional thin sheath),
(b) $\lambda < a < 4\lambda_D$ (collisional thick sheath),
(c) $4\lambda_D < \lambda < a$ (collisionless thin sheath: dense case).

2. Boltzmann Plot Method

The Boltzmann plot method uses the following equation given as the [6]:

$$\ln\left(\frac{\lambda \cdot \epsilon(\lambda)}{c \cdot A \cdot g}\right) = -\frac{E_u}{T_{ex}} + K, \tag{2}$$

where K=ln($hn_i/4\pi Z_i$). n_i is the population density of species i, λ is the wavelength, ϵ is the volumetric emission coefficient of the line, c is the speed of light, A is the transition probability per unit time, g is the statistical weight of the upper excited state, E_u is the energy of the upper excited state, T_{ex} is the excitation temperature, h is the Planck's constant, and Z_i is the partition function calculated at T_{ex}. The variable related to the K is constant and is independent of the selected spectral line. When we know the values of A and g for each spectral line, if the left-hand side of Eq. (2) is plotted against E_u, the plot is a straight line with a slope which is proportional to T_{ex}^{-1} for the case of LTE. However, for the case of the partial LTE, the plot exhibits two straight lines, and an accurate temperature can be calculated if we know the density of the ground state. In order to apply the more accurate Boltzmann plot method, we have at least five spectral lines, and we should use an electron temperature which is not the excitation temperature from the case of non-LTE plasmas. One can still see the non-LTE properties through the Boltzmann plot method because the excitation temperature is related to the kinetic temperatures of the free electrons and is sensitive to the non-equilibrium [16]. When the plasma state is in partial LTE in low pressure, we should consider the upper excited levels, as well as the highest level, for calculating the electron temperature from excitation temperatures when using the MTE model [17,18], which is proposed for calculating the electron temperature for a multi-temperature plasma (T_e, T_g, T_{ex}, *etc.*) when the excitation temperatures of the atoms and the ions are equivalent [19,20].

III. EXPERIMENTAL SETUP

The experimental apparatus is composed of a discharge chamber (36 cm in diameter, 1 m in length), a DC power supply, a spectroscopy system, a fast scanning probe system with a single probe. Figure 1 shows a schematic diagram of the system. The spray gun is a non-transferred arc-type system that contains a cathode and a anode inside [21]. The anode is made of oxygen-free copper that has a high conductivity and purity (64

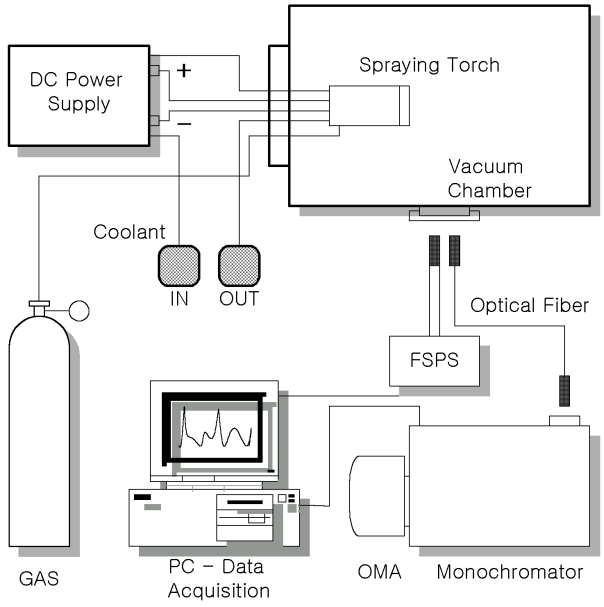

Fig. 1. Schematic diagram of a low-pressure plasma-spraying system.

mm in diameter, 40 mm in the height) while the cathode is made of thoriated tungsten (8 mm in diameter, 6 mm in height). The anode and the cathode are installed along a coaxial line and are cooled by water in order to prevent overheating. The fast scanning probe system, which is driven by a pneumatic cylinder with stroke of 5∼10 cm, measures the electron temperature and the plasma density by using a single probe (0.25 mm in radius, 1 mm in length). The spectroscopy system is composed of a monochromator, an optical multichannel analyzer (OMA), and an optical fiber. The monochromator has a 500-mm focal length and a 0.05-nm resolution. The spectral response of the OMA is 300∼900 nm at 1024×128 pixels.

Experiments were performed at a base pressure of 50 mtorr and a working pressure of 50 torr. After injection of the Ar gas, the spraying plasma (about 1 cm in diameter, 5 cm in length) was generated using 800 W of DC power (40 A and 20 V). Also, the non-thermal properties of plasma were measured by using the fast scanning probe system and the optical emission spectroscopy system. The fast scanning probe system with a single probe had an average operating speed of 0.4∼0.7 m/sec and a maximum speed of 2.2 m/sec, was used to measure the plasma density and the electron temperature. The optical emission spectroscopy system with a monochromator received the light emitted from the spraying plasma. The measured signals were interpreted by using the Boltzmann plot method.

IV. EXPERIMENTAL RESULTS

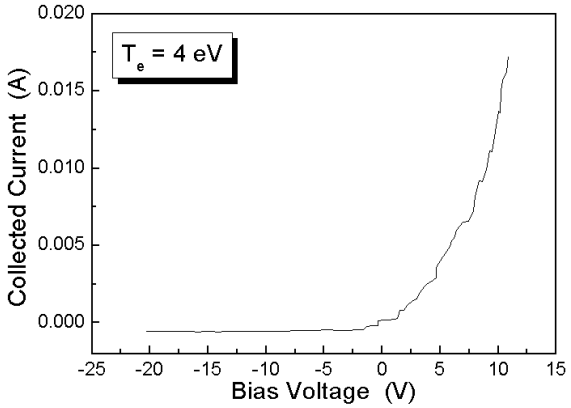

Fig. 2. I-V curve at the center (r=0 mm) of a low-pressure spraying plasma as determined by using a single probe.

Figures 2 and 3 show the current-voltage (I-V) curve and the electron energy distribution function (EEDF) measured by placing the single probe at the center (r=0 mm). The EEDF ($f_e(E)|_{E=eV}$) can be calculated from the second derivative of I-V curve; also, the plasma density (n_e) and the effective electron temperature (T_{eff}) can be calculated from integration of the EEDF [22–24]:

$$f_e(E)|_{E=eV} = \frac{4}{A_p e^2}\left(\frac{m_e V}{2e}\right)^{1/2}\frac{d^2 I_e}{dV^2}, \tag{3}$$

$$n_e = \int_0^\infty f_e(E)|_{E=eV} dV, \tag{4}$$

$$T_{eff} = 2/(3n_e)^{-1}\int_0^\infty E f_e(E)|_{E=eV} dV, \tag{5}$$

where E is the electron energy, A_p is the probe area, e is the electron charge, m_e is the electron mass, V is the difference between the plasma potential and probe bias, and I_e is the electron current to the probe. According to Eqs. (3), (4) and (5), the electron temperature can be explained by using a one-temperature

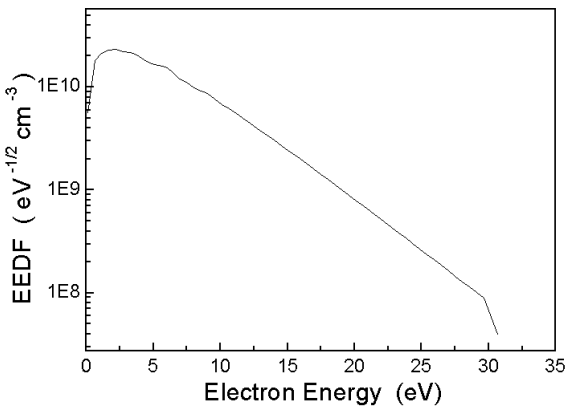

Fig. 3. Electron energy distribution function (EEDF) at the center (r=0 mm) of a low-pressure spraying plasma as determined by using a single probe.

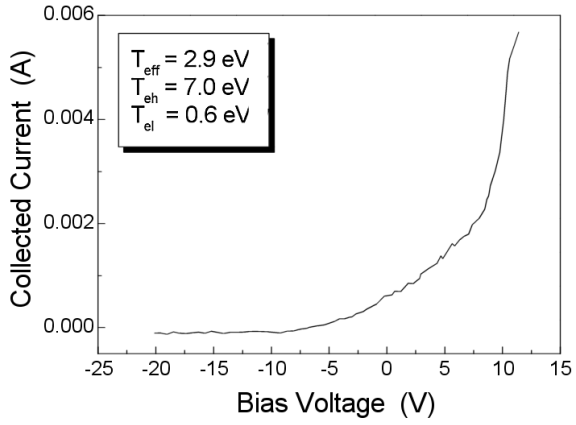

Fig. 4. I-V curve at the surface (r=4 mm) of a low-pressure spraying plasma as determined by using a single probe.

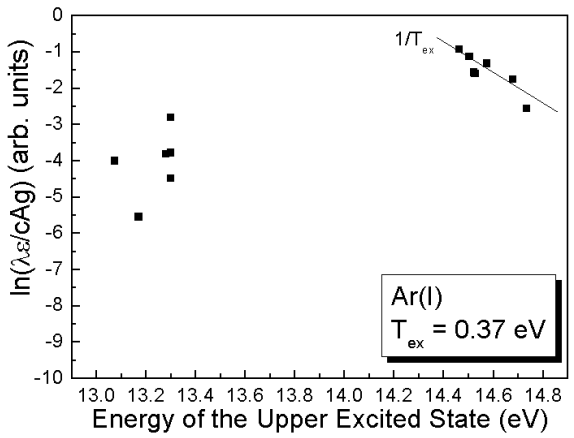

Fig. 6. Excitation temperature of the atomic (Ar(I)) line.

model (T_e=4 eV) or a Maxwellian model, and according to the collisionless theory, plasma density in Figs. 2 and 3 is 1.88×10^{11} cm^{-3}. Similarly, Figs. 4 and 5 show the I-V curve and the EEDF measured by a single probe at the surface (r=4 mm). In this case, the EEDF can be represented by using a two-temperature model (T_{eff}=2.9 eV, T_{elow}=0.6 eV, T_{ehigh}=7.0 eV) or a bi-Maxwellian, and according to the collisionless theory, the plasma density is 7.79×10^{10} cm^{-3} (n_{elow}=5.25×10^{10} cm^{-3}, n_{ehigh}=2.54×10^{10} cm^{-3}). The above plasma density and electron temperature indicate that collsional theory must be considered because $4\lambda_D$ is calculated to be 1.37×10^{-2} cm at the center and 1.81×10^{-2} cm at the surface. Also electron-neutral mean free path is calculated to be 4.14×10^{-4} cm at a neutral temperature of 1000 K.

The plasma density, according to the collisional theory, is given by [15]

$$I_i = 2\pi L e \mu_i n_0 (kT_e + kT_i) \frac{1}{\ln\left(\frac{\pi L}{4a}\right)}, \qquad (6)$$

where I_i is the ion current, L is the probe length, n_0 is the plasma density far from the probe, and T_i is the ion temperature. We assumed an ion temperature of 0.2∼0.5 eV (about 1 eV above the electron temperature) because Eq. (6) needs T_i. With assumption, the plasma density is calculated to be 1.57×10^{13} cm^{-3} at the center and 5.14×10^{12} cm^{-3} (n_{elow}=3.47×10^{12} cm^{-3}, n_{ehigh}=1.67×10^{12} cm^{-3}) at the surface. Also, from the above plasma density and electron temperature, $4\lambda_D$ is calculated to be 1.48×10^{-3} cm at the center and 2.19×10^{-3} cm at the surface. Consequently, collsional thin theory is proper for analyzing of our plasma because of $\lambda < 4\lambda_D < a$ [(a) of Case II in Sec. II].

Figures 6 and 7 show results plotted by using the Boltzmann plot method after classifying the intensity into the atomic line (Ar(I)) intensity and the ionic line(Ar(II)) intensity. The intensity was measured from the light emitted from the center of the spraying plasma. The atomic line of Ar was fitted with two straight lines, and the ionic line of Ar was fitted with one straight line. The atomic line and the ionic line of Ar each have a different excitation temperature. Therefore, for

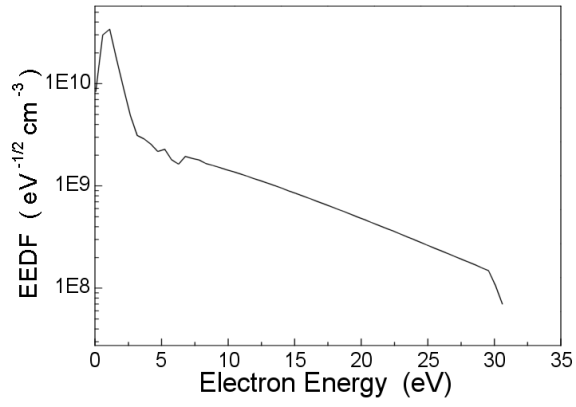

Fig. 5. Electron energy distribution function (EEDF) at the surface (r=4 mm) of a low-pressure spraying plasma as determined by using a single probe.

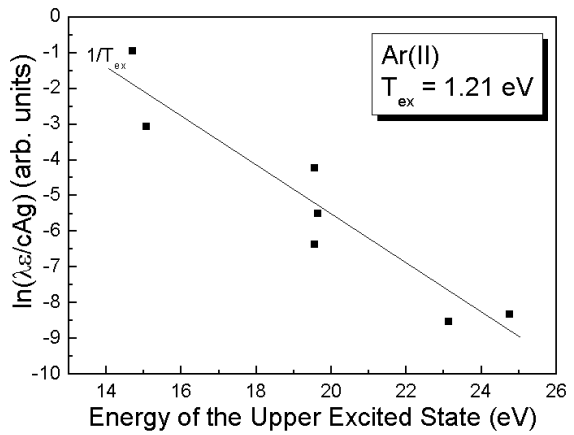

Fig. 7. Excitation temperature of the ionic (Ar(II)) line.

a low-pressure spraying plasma (50 torr) the multi-thermodynamic equilibrium (MTE) model must be applied [11]. From the atomic line of Ar, plasma can be described as a recombining plasma composed of a warm plasma and a cold Ar gas [25].

V. CONCLUSIONS

The plasma density and the electron temperature were measured by using the single probe in a fast scanning probe system. The two-temperature model could describe the temperature of electrons, which had non-isothermal properties. The electron density was revised by using the collisional plasma theory described before. In a low-pressure spraying plasma, the non-isothermal characteristics of the electrons are due to the rapid variation of the plasma density. Also, the Boltzmann plot method explains the non-LTE effects by the analyzing the intensities of the atomic and the ionic spectral lines from the plasma, which were measured by using a spectroscopic system. For a low-pressure spraying plasma, the MTE model seems to be appropriate because the atomic and the ionic lines of Ar each have a different excitation temperature.

ACKNOWLEDGMENTS

The authors would like to thank Yong-Sup Choi and Kyung-Chul Kim for their assistance during the experiment. This work was supported by the Korea Science and Engineering Foundation and by the Brain Korea 21 project.

REFERENCES

[1] P. Fauchais and A. Vardelle, IEEE Trans. Plasma Sci. **25**, 1258 (1997).
[2] C. Oberlin, High Temp. Chem. Process. **3**, 719 (1994).
[3] M. Back and G. Gruchov, Pure Appl. Chem. **64**, 665 (1992).
[4] H. J. Bebber, High Temp. Chem. Process. **3**, 665 (1994).
[5] J. H. Zaat, Ann. Rev. Mater. Sci. **13**, 9 (1983).
[6] P. Fauchais, J. F. Coudert and M. Vardelle, *Plasma Diagonostics*, edited by O. Auciello and D. L. Flamm (Academic Press, San Diego, 1989), Vol. 1, Chap. 2, p. 349.
[7] B. J. LEE and H. Koinuma, J. Korean Phys. Soc. **39**, 998 (2001).
[8] W. L. Weise, D. E. Kelleher and D. R. Pacquette, Phys. Rev. A **6**, 1132 (1972).
[9] W. Weise, *The Physics of Ionized Gases*, edited by G. Pichler (Institute of Physics, Zagreb, 1983), p. 435.
[10] T. L. Eddy, J. Quant. Spectrosc. Radiat. Transfer **33**, 197 (1985).
[11] T. L. Eddy and A. Sadghinasab, IEEE Trans. Plasma Sci. **16**, 444 (1988).
[12] F. F. Chen, *Plasma Diagnostic Techniques*, edited by R. H. Huddlestone and S. L. Leonard (Academic Press, New York, 1965), Chap. 4, p. 113.
[13] I. H. Hutchinson, *Principles of Plasma Diagonostics* (Cambridge Univ. Press, Cambridge, 1987), Chap. 3, p. 50.
[14] P. M. Chung, L. Talbot and K. T. Touryan, *Electric Probes in Stationary and Flowing Plasmas: Theory and Applications* (Springer-Velrag, New York, 1975).
[15] D. N. Ruzic, *Electric Probes for Low Temperature* (AVS Monograph Series, New York, 1994).
[16] C. O. Laux, Stanford Univ. HTGL Report T-288 (1993).
[17] T. L. Eddy, E. Pfender and E. R. G. Eckert, IEEE Trans. Plasma Sci. **1**, 31 (1973).
[18] T. L. Eddy, C. J. Cremers and H. S. Hsia, J. Quant. Spectrosc. Radiat. Transfer **17**, 287 (1977).
[19] T. L. Eddy, IEEE Trans. Plasma Sci. **4**, 103 (1976).
[20] H. Shindo and Imazu, J. Quant. Spectrosc. Radiat. Transfer **23**, 605 (1980).
[21] S. H. Hong, ITEP Report A00-901-1106-11-3-3 (1993).
[22] L. J. Mahoney, A. E. Wendt, E. Barrios, C. J. Richards and J. L. Shohet, J. Appl. Phys. **76**, 2041 (1993).
[23] H. Singh and D. B. Graves, J. Appl. Phys. **47**, 4098 (2000).
[24] V. A. Godyak, R. B. Piejak and B. M. Alexandrovich, J. Appl. Phys. **73**, 3657 (1993).
[25] M. C. Quinterro, A. Rodero, M. C. Garcia and A. Sola, Appl. Spectrosc. **51**, 778 (1997).